# Supporting Information

## Chen et al. 10.1073/pnas.1012348107

### SI Materials and Methods

**Constructs of Site-Directed CesA1 Mutants.** pCesA1-gateway, a Ti plasmid containing the CesA1 promoter flanking the att sites, was constructed by replacing the 35S promoter of pMDC32 with a HindIII-AscI fragment containing the CesA1 promoter. The CesA1 promoter was amplified from *Arabidopsis* genomic DNA using primers 5′-atgaaagcttttaagttaagtgtttgttctttttactgagaa-3′ and 5′- ataggcgcgcccgcagccaccgacacacag-3′, which introduce HindIII and AscI restriction sites, respectively. HindIII-AscI fragments from pMDC32 and the amplified CesA1 promoter were ligated to give pCesA1-gateway. The CesA1 ORF from pMW2 (CesA1 cDNA clone with an introduced AatII site) was amplified using primers 5′-ggggacaagtttgtacaaaaaagcaggcttggtggctgcgatggaggcca-3′ and 5′-ggggaccactttgtacaagaaagctgggtacataagtgtgagtctaacaagc-ttt-3′, which add attB1 and attB2 sites flanking CesA1 cDNA, respectively. The resulting PCR product was recombined into pDONR/Zeo to give pCesA1-donr by using Gateway reactions (Invitrogen). All the constructs were sequenced to ensure no error.

pCesA1-donr was used as the template for site-directed mutagenesis with the QuikChange II site-directed mutagenesis kit (Stratagene). Mutagenic oligonucleotide primers were designed to produce changes that led to the introduction of the following amino acid substitutions: S162A, S162E, T165A, T165E, T166A, T166E, S167A, S167E, S686A, S686E, S688A, and S688E (Table S2). The mutants of pCesA1-donr were used to introduce mutagenized CesA1 genes into pCesA1-gateway using Gateway reactions. For each site-directed mutagenesis, a unique restriction site was introduced and used to confirm the presence of successful substitution.

**Tissue and Cell Length Measurements.** To grow seedlings, seeds were surface sterilized with dilute bleach and stratified at 4 °C for 2 d in 0.15% agar followed by 3 to 5 d on plates containing 0.5× MS mineral salts (Sigma) and 0.9% agar before being placed in darkness or in a continuous white light growth chamber (200 μmol·m$^{-2}$·s$^{-1}$) at 19 °C (permissive temperature) or 30 °C (restrictive temperature).

Images of 20 to 30 seedlings grown on vertically placed MS plates were captured by a scanner and the image files were analyzed by ImageJ to measure the lengths of primary roots or dark-grown hypocotyls.

For measurements of root epidermal cell length, 7-d-old light-grown seedlings were stained with 1 μg/mL of propidium iodide in water for 4 min, followed by several rinses in 1× PBS solution. Images of epidermal cells, located in the approximate middle of roots, were captured by a spinning-disk confocal microscope (1). Images of hypocotyl epidermal cells were obtained by using a Quanta 200 environmental scanning electron microscope (FEI) under a pressure of 130 Pa and a voltage of 12.5 kV with a low-vacuum detector. Images were processed with ImageJ to measure epidermal cell length. Between 120 and 150 cells were measured from four to six different roots for WT and each mutant. For hypocotyls, approximately 80 cells were measured from five different plants.

**Measurements of CESA Particle Velocity.** Two methods were used to measure labeled CESA complex velocities. First, individual tracks of CESA complex movement were analyzed using the Multiple Kymograph plug-in for ImageJ (J. Rietdorf and A. Seitz, European Molecular Biology Laboratory, Heidelberg, Germany), as previously described (2).

Second, YFP::CESA particles in large image regions were tracked on an automated basis using the spots tool in Imaris software (version 6.2; Bitplane). Analysis regions were set to include the majority of the optical cross section through the cortex of each analyzed cell, avoiding regions with high proplastid autofluorescence. The target spot size was set to 250 nm (approximately two pixels at the sampled resolution). The default quality score was accepted for spot detection and the connected components algorithm applied to generate tracks. Tracks with durations below 60 s were discarded and the remaining tracks analyzed for mean displacement angle relative to the long axis of the cell (as estimated by eye), and for mean velocity (as estimated by total x and y displacement of each track). Individual particles persisting for longer than 60 s were tracked, and their X and Y displacements and durations recorded. The major direction of particle flux was calculated by summing the displacements of all recorded particles:

$$\text{Let } \vec{v}_i = \langle \Delta x_i, \Delta y_i \rangle \qquad \text{[S1]}$$

$$\vec{V} = \sum_{i=1}^{n} \vec{v}_i \qquad \text{[S2]}$$

This vector was normalized to a unit vector by dividing by its length (Eq. S3). This unit vector represents an axis of bias for overall particle movement.

$$\vec{A} = \frac{\vec{V}}{\|V\|} \qquad \text{[S3]}$$

Individual track velocity vectors were decomposed into two component vectors, one parallel to the major axis and one orthogonal to the major axis. Tracks were classified into two groups based on whether the parallel component was aligned with or against the major axis of CESA movement. In some cases, the major direction of particle flux calculation failed and tracks were grouped by analyzing the distribution of track angles, followed by assignment of particles into two groups based on the position of the two major minima in the angular distribution (Fig. S3). In the latter case, the group with the greater number of tracks was designated the "with" group and that with fewer tracks designated the "against" group. All statistical analyses of velocities observed in single cells were performed using a two-tailed *t* test that assumed equal variances among compared populations. Summary values for each genotype or experimental treatment were calculated as the means of the single-cell means.

1. Paredez AR, Somerville CR, Ehrhardt DW (2006) Visualization of cellulose synthase demonstrates functional association with microtubules. *Science* 312:1491–1495.

2. Paredez AR, Persson S, Ehrhardt DW, Somerville CR (2008) Genetic evidence that cellulose synthase activity influences microtubule cortical array organization. *Plant Physiol* 147:1723–1734.

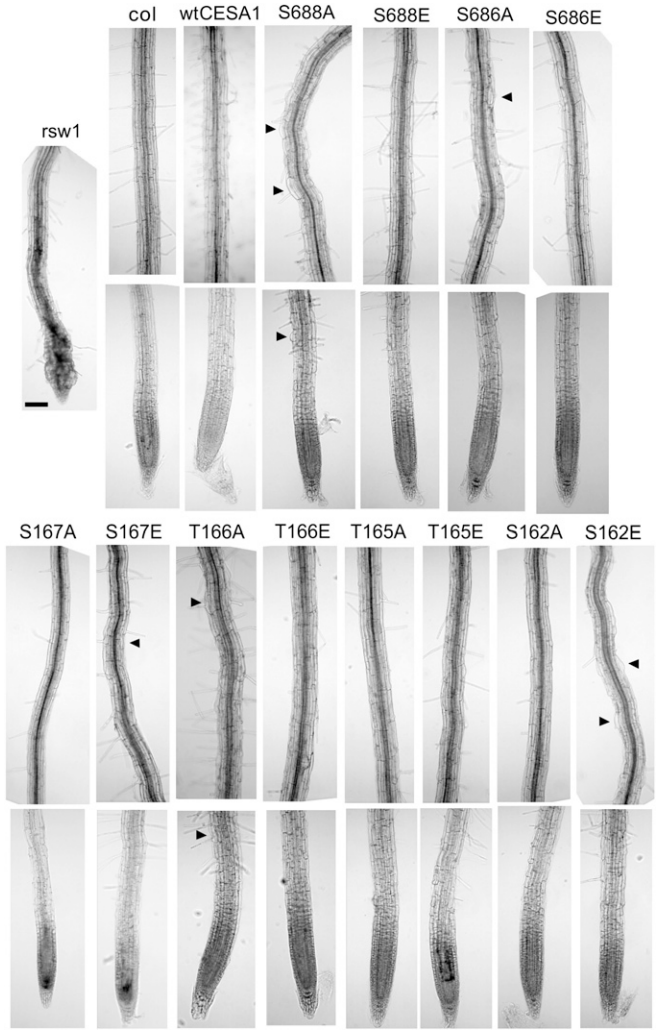


**Fig. S1.** Roots of Col-0, *rsw1*, and *rsw1* transgenic lines containing WT CESA1 or *cesA1*$^{P}$ mutants. Seedlings were grown in continuous light (200 μmol/m$^2$/s) on vertical 0.5× MS agar plates at 30 °C for 7 d. (Scale bar: 100 μm.)

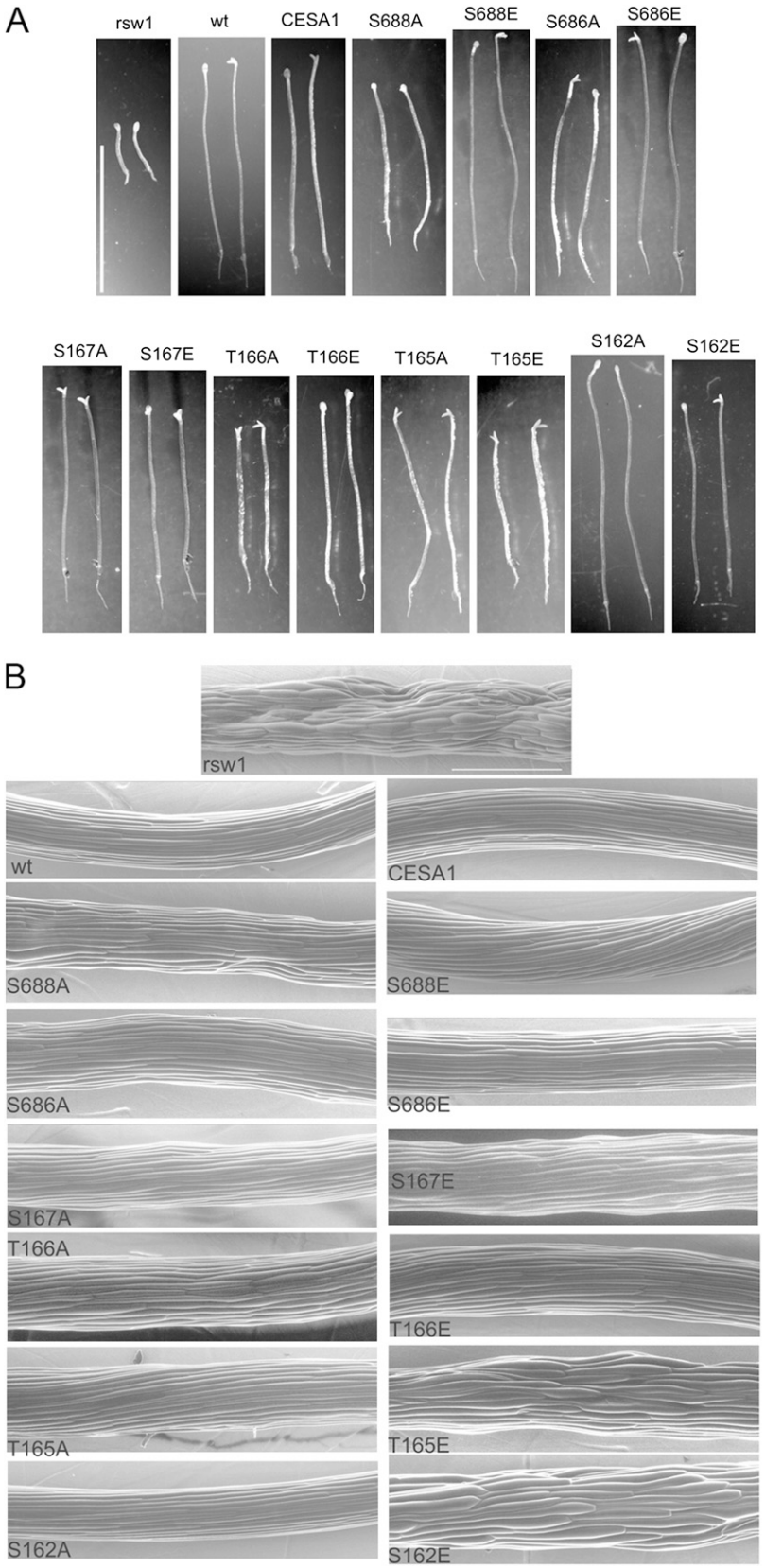


**Fig. S2.** Dark-grown seedlings of Col-0, *rsw1*, and *rsw1* transgenic lines containing WT CESA1 cDNA or *cesA1*$^{p}$ mutants (*A*), and scanning EM images of their enlarged hypocotyls (*B*). Seedlings were grown on vertical 0.5× MS agar plates at 30 °C for 5 d in darkness.

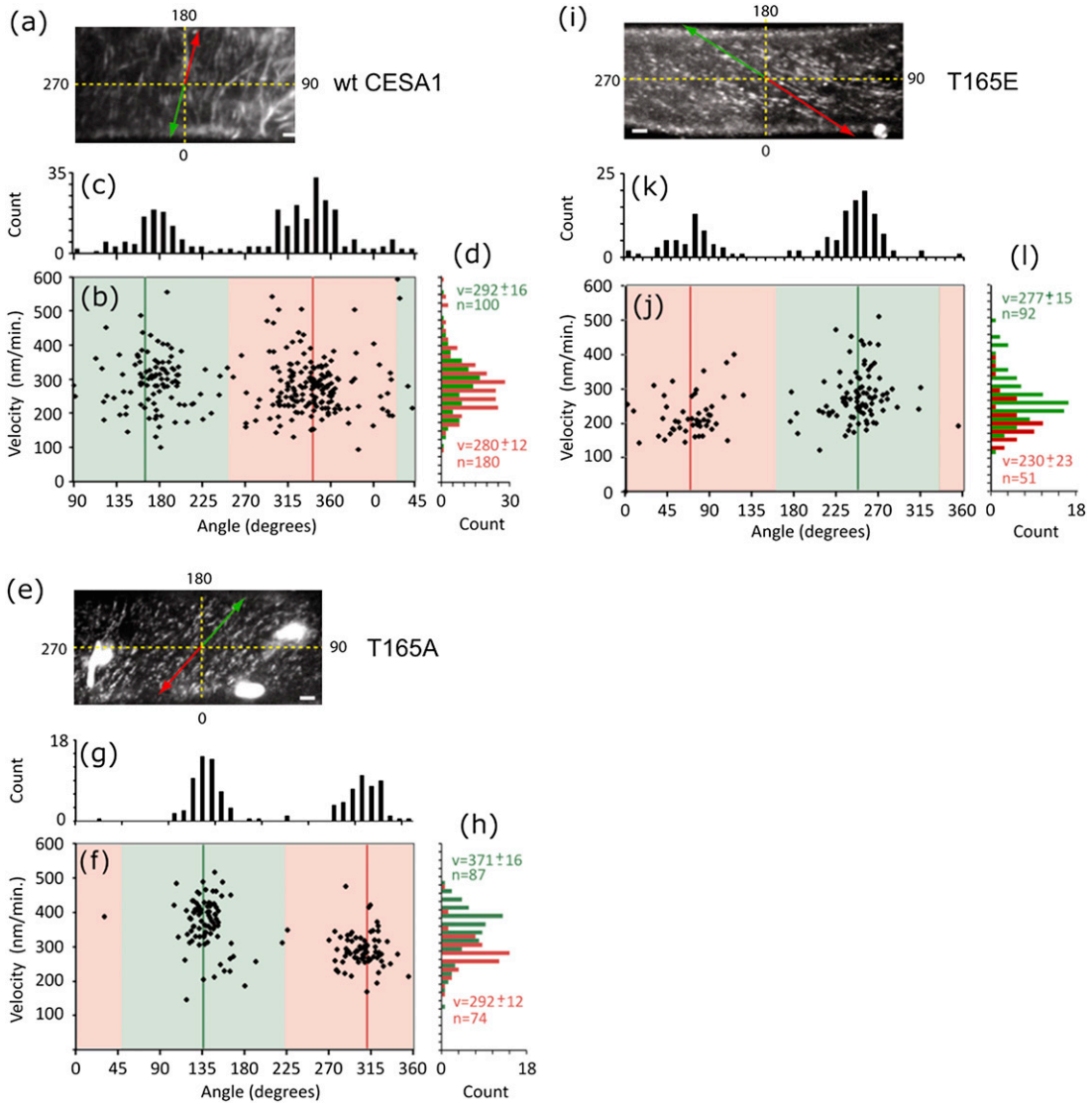


**Fig. S3.** Analysis of bidirectional movement of CESA complexes in the WT, T165A, and T165E transgenic lines using the spots tool in Imaris software. Time-lapse confocal images of YFP::CESA6 in hypocotyl cells of etiolated seedlings grown at restrictive temperature for 2 d were used to measure CESA particle velocity at 29 °C. To analyze bidirectional movement of CESA particles, we defined and calculated the major direction of particle flux and classified CESA particles as moving either with or against the major axis as described in the section of (*Materials and Methods* and *SI Materials and Methods*). (*A*, *I*, and *E*) Average time projections of 61 frames representing 5 min. Red and green arrows indicate two opposite directions of particle movement relative to the major axis (Fig. S4 *A* and *B*). (*B*, *J*, and *F*) Velocity and direction distribution of CESA particles moving with or against the major axis as indicated by different background colors. Red and green lines indicate directions of the major axis. (*C*, *K*, and *G*) Histograms of particle movement directions. (*D*, *H*, and *L*) Histograms of particle velocities.

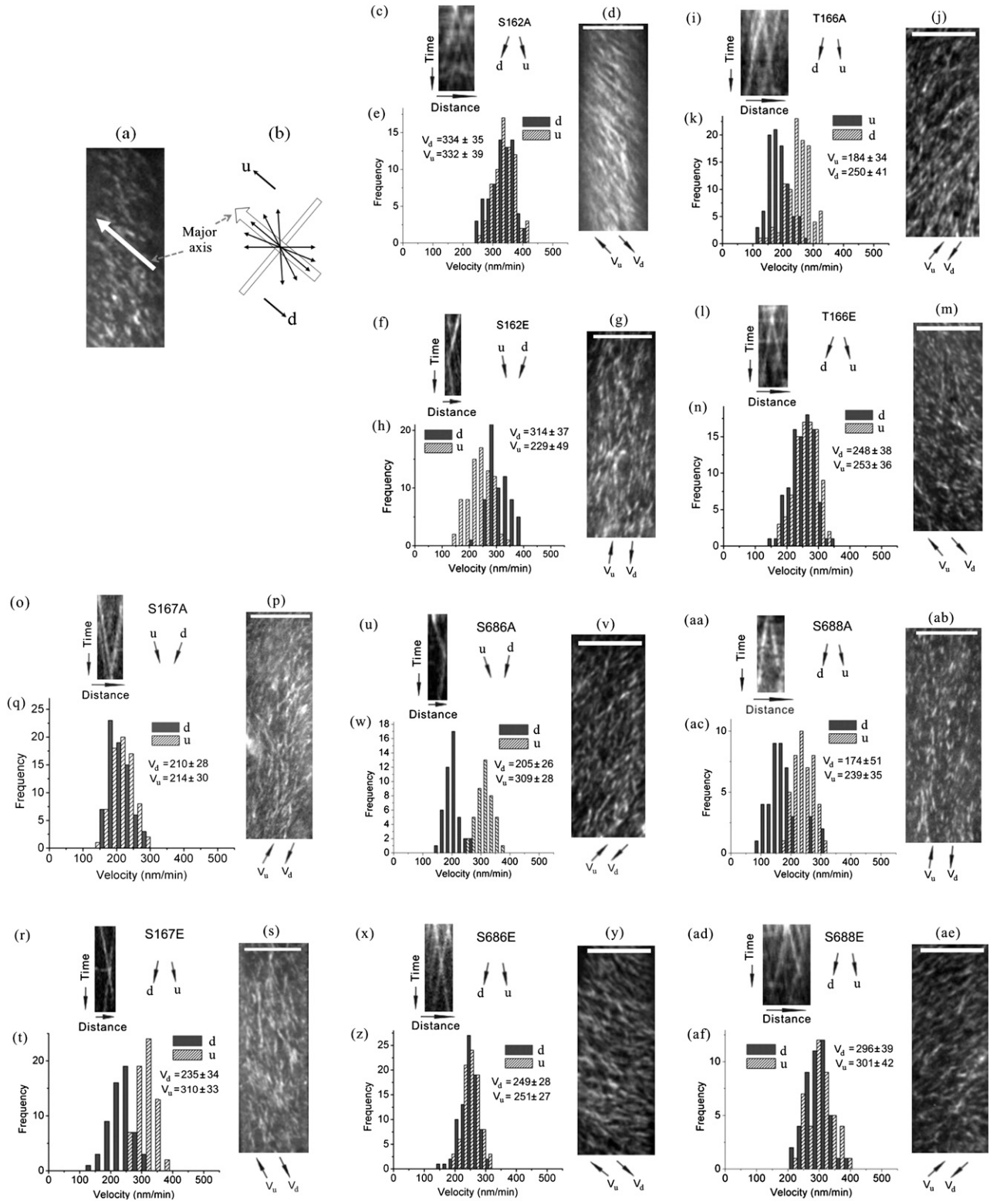


**Fig. S4.** Kymograph analysis of bidirectional movement of CESA complexes in *cesA1*$^{P}$ mutant lines. The data for the WT, T165A, and T165E transgenic lines is presented in Fig. 4. To analyze bidirectional movement of CESA particles, we defined the average axis of CESA particle movement in a given image series of a cell as the major axis. (*A*) An example of major axis (white arrow) of an image series. Average time projections show directions of CESA particle trajectories. (*B*) CESA particles were classified as moving in upward (u) or downward (d) direction along the major axis. This figure presents the data for the mutations at the residues of S162, T166, S167, S686, and S688. The data for WT, T165A, and T165E is presented in Fig. 4. Time-lapse confocal images of YFP::CesA6 in hypocotyl cells of etiolated seedlings grown at restrictive temperature for 2 d were used to measure CESA particle velocity at 29 °C. (*C*, *F*, *I*, *L*, *O*, *R*, *U*, *X*, *AA*, and *AD*) Representative kymograph displays effects of mutations on bidirectional particle translocation. (*D*, *G*, *J*, *M*, *P*, *S*, *V*, *Y*, *AB*, and *AE*) Average time projections of 61 frames representing 5 min. (*E*, *H*, *K*, *N*, *Q*, *T*, *W*, *Z*, *AC*, and *AF*) Histograms of particle velocities calculated from kymograph analysis of 100 to 200 particles from three to six cells of a single seedling. (Scale bars: 10 μm in *D*, *G*, *J*, *M*, *P*, *S*, *V*, *Y*, *AB*, and *AE*.)

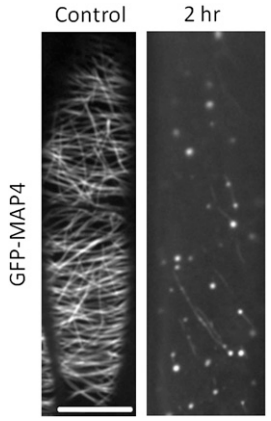


**Fig. S5.** Effects of oryzalin on microtubule organization. Confocal images of cortical microtubules labeled with GFP::MAP4 in hypocotyl cells of 2-d-old etiolated *Arabidopsis* seedlings grown at 30 °C. (*A*) Control treatment with 0.02% methanol for 2 h at 29 °C. (*B*) Treatment with 20 μM oryzalin at 29 °C for 2 h cleared most microtubules from the cortex. (Scale bar: 10 μm.)

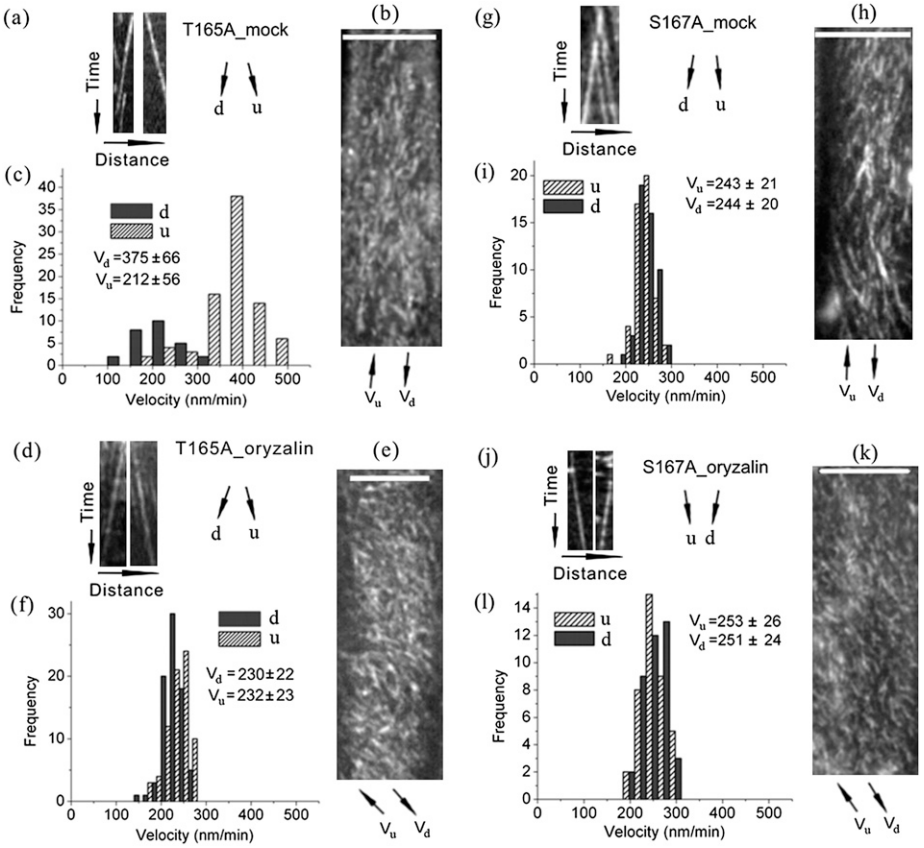


**Fig. S6.** Effects of oryzalin on bidirectional movement of CesA complexes in the T165A and S167A transgenic lines. Time-lapse confocal images of YFP::CESA6 in hypocotyl cells of 2-d-old etiolated plants grown at 30 °C were used to measure CESA particle velocity. u and d represent two opposite directions of particle movement relative to the major axis (Fig. S4 *A* and *B*). (*A–C* and *G–I*) Control treatment with 0.02% methanol or DMSO at 29 °C for 2 to 3 h. (*D–F* and *J–L*) Treatment with 20 μM oryzalin at 29 °C for 2 to 3 h. (*A*, *D*, *G*, and *J*) Representative kymograph displaying effects of oryzalin treatment on bidirectional particle translocation. (*B*, *E*, *H*, and *K*) Average time projections of 61 frames representing 5 min. (*C*, *F*, *I*, and *L*) Histograms of particle velocities calculated from kymograph analysis of 100 to 200 particles from three to six cells of a single seedling. (Scale bars: 10 μm in *B*, *E*, *H*, and *K*.)

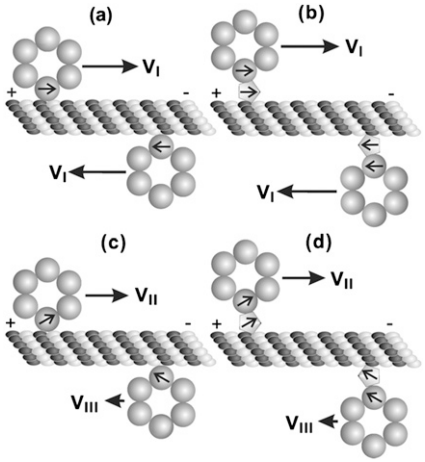


**Fig. S7.** Potential mechanisms for the directional asymmetry of CESA velocity and distribution in CESA1 mutant lines. We propose that each cortical microtubule, or microtubule bundle, has lateral interactions with CESA complexes through the cytosolic domains of CESA complexes (*A* and *C*) or molecular linkers that interact with the cytosolic domains (*B* and *D*), leading to organization of two linear arrays of CESA, one on either side of the microtubule or bundle. To better illustrate microtubule–CESA complex interactions, we schematize only microtubule subunit structure. (*A* and *B*) The polarity of microtubule structure or asymmetry of CESA complex structure and the confinement of the CESA complex orientation by its association with the plasma membrane would result in asymmetrical lateral interactions between microtubules and CESA complexes on each side of the microtubule. In the WT line, microtubule integrity has no effect on CESA velocity, so it is presumed that the affects of these asymmetric lateral interactions on complex velocity are small. (*C* and *D*) In transgenic lines such as T165E and T165A, the mutations result in a modification of CESA velocity that is dependent on microtubule interaction. Because these lateral interactions are predicted to differ on either side of the microtubule, this feedback on complex velocity may also be asymmetric, resulting in a velocity differential on either side of the microtubule, thus creating two complex velocity classes. $V_I$, $V_{II}$, and $V_{III}$ represent differences in the rate of CESA complex movement along microtubules.

**Table S1. Measurements of the rate of bidirectional movement of CESA complexes and cellulose contents in the various *cesA1*$^{P}$ mutants**

| Mutant | $V_d$ or $V_m$, nm/min* | $V_u$ or $V_p$, nm/min* | Mean $\Delta V \pm$ SD* | *P* value range* | Cellulose content† |
|---|---|---|---|---|---|
| A1wt1 | 243 ± 25 | 244 ± 19 | 7 ± 6 | 0.1–0.9 | 191 ± 8 |
| S162A | 275 ± 38 | 278 ± 38 | 8 ± 5 | 0.3–0.9 | 238 ± 8 |
| S162E* | 213 ± 17 | 246 ± 15 | 33 ± 3 | $2 \times 10^{-4}$ to 0.005 | 157 ± 2 |
| T165A* | 287 ± 11 | 335 ± 22 | 48 ± 13 | $1 \times 10^{-7}$ to 0.003 | 195 ± 5 |
| T165E* | 204 ± 25 | 245 ± 34 | 41 ± 24 | $8 \times 10^{-19}$ to 0.009 | 170 ± 4 |
| T166A* | 223 ± 36 | 268 ± 40 | 45 ± 14 | $2 \times 10^{-10}$ to $4 \times 10^{-4}$ | 171 ± 4 |
| T166E | 237 ± 21 | 239 ± 22 | 7 ± 7 | 0.1–0.9 | 212 ± 9 |
| S167A | 221 ± 23 | 222 ± 24 | 5 ± 4 | 0.1–0.8 | 225 ± 5 |
| S167E* | 215 ± 29 | 277 ± 44 | 62 ± 26 | $1 \times 10^{-17}$ to $7 \times 10^{-4}$ | 175 ± 7 |
| S686A* | 214 ± 19 | 256 ± 22 | 42 ± 6 | $5 \times 10^{-12}$ to 0.002 | 175 ± 5 |
| S686E | 268 ± 33 | 271 ± 35 | 4 ± 2 | 0.5–0.9 | 204 ± 9 |
| S688A* | 186 ± 31 | 235 ± 26 | 49 ± 27 | $7 \times 10^{-7}$ to 0.006 | 168 ± 3 |
| S688E | 277 ± 39 | 273 ± 43 | 8 ± 8 | 0.1–0.8 | 214 ± 7 |
| Col-0 | ND | ND | ND | ND | 201 ± 8 |
| rsw1 | ND | ND | ND | ND | 107 ± 2 |
| T165A (mock)‡ | 263 ± 18 | 333 ± 47 | 70 ± 38 | $4 \times 10^{-15}$ to 0.006 | ND |
| T165A (oryzalin)§ | 246 ± 6 | 241 ± 10 | 7 ± 1 | 0.3–0.7 | ND |
| T165E (mock)‡ | 184 ± 21 | 234 ± 17 | 50 ± 24 | $1 \times 10^{-6}$ to 0.01 | ND |
| T165E (oryzalin)§ | 198 ± 21 | 201 ± 18 | 7 ± 3 | 0.5–0.9 | ND |
| S167A (mock)‡ | 227 ± 22 | 227 ± 26 | 5 ± 4 | 0.2–0.9 | ND |
| S167A (oryzalin)§ | 232 ± 9 | 234 ± 7 | 4 ± 3 | 0.2–0.9 | ND |

ND, not determined.

*As in the kymograph analysis, we defined the average trajectory of CESA particle movement in a given image series of a cell as the major axis and classified CESA particles as moving in upward or downward direction along the major axis within 90° bins centered around 0° and 180° (Fig. S4 *A* and *B*). Velocity differences between the two populations of particles (upward or downward) in a given cell were assessed by a *t* test and the range of *P* values from different cells is shown (six to 14 cells from four to seven seedlings for each transgenic line). For the transgenic lines [T165A (mock) and T165E (mock)] that showed significant velocity discrepancy, the two populations of CESA particles from different cells were further grouped as either slow-moving (denoted as m) or fast-moving (denoted as p) and mean velocities ($V_m$ and $V_p$) were then calculated and shown as means ± SD of measurements of different cells. For WT and the other transgenic lines that didn't show velocity discrepancy, however, these two populations of CESA particles were grouped again according to their upward (u) and downward (d) directions of movement along the major axis (Fig. S4 *A* and *B*).

†Cellulose content in the root of light-grown seedlings was measured as TFA-insoluble glucose, and value is the mean of at least three measurements with SEs. Values expressed as μg cellulose per mg plant dry weight.

‡Intact seedlings of a transgenic line were treated with 0.2% methanol or DMSO at 29 °C for 2–3 h before measurements.

§Intact seedlings of a transgenic line were treated with 0.2% methanol or DMSO plus 20 μM of oryzalin at 29 °C for 2–3 h before measurements.

**Table S2. Primers used for site-directed mutagenesis**

| Mutation | Primers* | Restriction sites being added |
|---|---|---|
| S162A | gcacgcctgatacacaaGCAgtgcgaactacatcagg<br>cctgatgtagttcgcacTGCttgtgtatcaggcgtgc | BtsI |
| S162E | cgcacgcctgatacacaaGAGgtTcgaactacatcaggtcc<br>ggacctgatgtagttcgAacCTCttgtgtatcaggcgtgcg | Bst BI |
| T165A | cacaatctgtgcgaGCGacatcaggtcctttggg<br>cccaaaggacctgatgtCGCtcgcacagattgtg | AhdI |
| T165E | cacaatctgtgcgGGAGacatcaggtcctttgggtccttctg<br>cagaaggacccaaaggacctgatgtCTCCcgcacagattgtg | FauI |
| T166A | ctgtgcgaactGCGtcaggtcctttgggtcc<br>ggacccaaaggacctgaCGCagttcgcacag | HgaI |
| T166E | cacaatctgtgcgaactGAAtcCggtcctttgggtccttc<br>gaaggacccaaaggaccGgaTTCagttcgcacagattgtg | BsaWI |
| S167A | ctgtgcgaactacaGCTggtcctttgggtccttc<br>gaaggacccaaaggaccAGCtgtagttcgcacag | PvuII |
| S167E | ctgtgcgaactacaGAGggtcctttgggtccttctgac<br>gtcagaaggacccaaaggaccCTCtgtagttcgcacag | SfcI |
| S686A | ggagaggcatcaacagaGCCgactccaatgctccac<br>gtggagcattggagtcGGCtctgttgatgcctctcc | BcgI |
| S686E | gaggagaggcatcaacagaGAAgactccaatgctccac<br>gtggagcattggagtcTTCtctgttgatgcctctcctc | BbsI |
| S688A | ggcatcaacagaagtgacGCCaatgctccac<br>gtggagcattGGCgtcacttctgttgatgcc | BsaHI |
| S688E | gaggagaggcatcaacagaagtgacGAGaatgctccactttttc<br>gaaaagtggagcattCTCgtcacttctgttgatgcctctcctc | BsmI |

*Mutagenized nucleotides in uppercase.

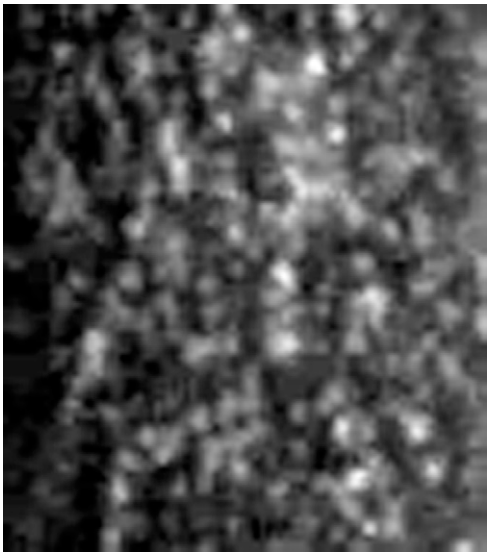

**Movie S1.** CESA complexes moving in linear tracks in opposite directions along microtubules were observed in WT controls.

Movie S1 (AVI)

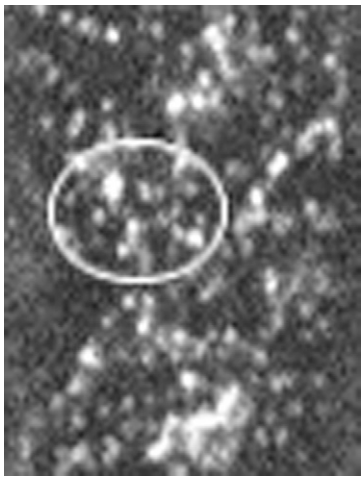

**Movie S2.** CESA complex movement in the T165A transgenic line. A cluster of CESA particles moving unidirectionally is highlighted in a circle in the sequential frames.

Movie S2 (AVI)